Implicitly-Defined Neural Networks for Sequence Labeling [*]

Michaeel Kazi, Brian Thompson
MIT Lincoln Laboratory
244 Wood St, Lexington, MA, 02420, USA
{first.last}@ll.mit.edu

Abstract

In this work, we propose a novel, implicitly-defined neural network architecture and describe a method to compute its components. The proposed architecture forgoes the causality assumption previously used to formulate recurrent neural networks and allow the hidden states of the network to coupled together, allowing potential improvement on problems with complex, long-distance dependencies. Initial experiments demonstrate the new architecture outperforms both the Stanford Parser and a baseline bidirectional network on the Penn Treebank Part-of-Speech tagging task and a baseline bidirectional network on an additional artificial random biased walk task.

1   Introduction

Feedforward neural networks were designed to approximate and interpolate functions. Recurrent Neural Networks (RNNs) were developed to predict sequences. RNNs can be 'unwrapped' and thought of as very deep feedforward networks, with each layer sharing the same set of weights. Computation proceeds one step at a time, like the trajectory of an ordinary differential equation when solving an initial value problem. The path of an initial value problem depends only on the current state and the current value of the forcing function. In a RNN, the analogy is the current hidden state and the current input sequence. However, in certain applications in natural language processing, especially those with long-distance dependencies or where grammar matters, sequence prediction may be better thought of as a boundary value problem. Changing the value of the forcing function (analogously, of an input sequence element) at any point in the sequence will affect the values everywhere else. The bidirectional network addresses this problem by allowing information to flow in both directions. However, each part can only consider information from one direction. In practice many algorithms require more than two passes through the data to determine an answer. We provide a different mechanism than the bidirectional network, with the motivation being a program which iterates over itself until convergence.

1.1   Related Work

Bidirectional, long-distance dependencies in sequences have been an issue as long as there have been NLP tasks, and there are many approaches to dealing with them.

Hidden Markov models (HMMs) (Rabiner, 1989) have been used extensively for sequence-based tasks, but they rely on the Markov assumption - that a hidden variable changes its state based only on its current state and observables. In finding maximum likelihood state sequences, the Forward-Backward algorithm can take into account the entire set of observables, but the underlying model is still local.

In recent years, popularity of the Long Short-Term Memory (LSTM) (Hochreiter and Schmidhuber, 1997) and variants such as the Gated Recurrent Unit (GRU) (Cho et al., 2014) has soared, as they enable RNNs to process long sequences without the problem of vanishing or exploding gradients (Pascanu et al., 2013). However, these models only allow for information/gradient information to flow in the forward direction.

The Bidirectional LSTM (b-LSTM) (Graves and Schmidhuber, 2005), a natural extension of (Schuster and Paliwal, 1997), incorporates past and future hidden states via two separate recurrent networks, allowing information/gradients to flow in both directions of a sequence. This is a very loose coupling, however.

In contrast to these methods, our work goes a step further, fully coupling the entire sequences of hidden states of an RNN. Our work is similar to (Finkel et al., 2005), which augments a CRF with long-distance constraints. However, our work differs in that we extend an RNN and uses Netwon-Krylov (Knoll and Keyes, 2004) instead of Gibbs Sampling.

2 The Implicit RNN (iRNN)

2.1 Traditional Recurrent Neural Networks

A typical recurrent neural network has a (possibly transformed) input sequence $[\xi_1, \xi_2, \ldots, \xi_n]$ and initial state h_s and iteratively produces future states:

$$
\begin{aligned}
h_1 &= f(\xi_1, h_s) \\
h_2 &= f(\xi_2, h_1) \\
&\ldots \\
h_n &= f(\xi_n, h_{n-1})
\end{aligned}
$$

The LSTM, GRU, and related variants follow this formula, with different choices for the state transition function. Computation proceeds linearly, with each next state depending only on inputs and previously computed hidden states.
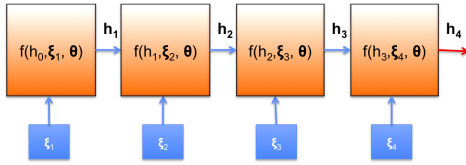

Figure 1: Traditional RNN structure.

2.2 Proposed Architecture

In this work, we relax this assumption by allowing $h_t = f(\xi_t, h_{t-1}, h_{t+1})$[1]. This leads to an implicit set of equations for the entire sequence of hidden states, which can be thought of as a single tensor H:

$$
H = [h_1, h_2, \ldots, h_n]
$$

This yields a system of nonlinear equations. This setup has the potential to arrive at nonlocal, whole sequence-dependent results. We also hope such a system is more 'stable', in the sense that the predicted sequence may drift less from the true meaning, since errors will not compound with each time step in the same way.

There are many potential ways to architect a neural network – in fact, this flexibility is one of deep learning's best features – but we restrict our discussion to the structure depicted in Figure 2. In this setup, we have the following variables:

data	X
labels	Y
parameters	θ

and functions:

implicit hidden layer definition	$H = F(\theta, \xi, H)$
loss function	$L = \ell(\theta, H, Y)$
input layer transformation	$\xi = g(\theta, X)$

Our implicit definition function, F, is made up of local state transitions and forms a system of nonlinear equations that require solving, letting h_s and h_e be boundary states:

---

[1] A wider stencil can also be used, e.g. $f(h_{t-2}, h_{t-1}, \ldots)$.

$$
\begin{aligned}
h_1 &= f(h_s, h_2, \xi_1) \\
&\ldots \\
h_i &= f(h_{i-1}, h_{i+1}, \xi_i) \\
&\ldots \\
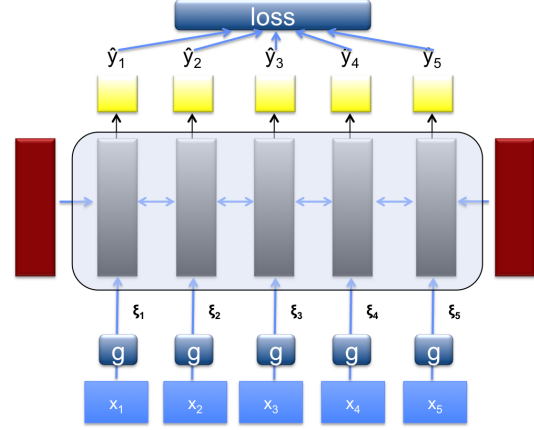h_n &= f(h_{n-1}, h_e, \xi_n)
\end{aligned}
$$

Figure 2: Proposed iRNN architecture

2.3 Computing the forward pass

To evaluate the network, we must solve the equation $H = F(H)$. We computed this via an approximate Newton solve:

$$
H_{n+1} = H_n - (I - \nabla_H F)^{-1}(H_n - F(H_n))
$$

Since $(I - \nabla_H F)$ is sparse, we apply Krylov subspace methods (Knoll and Keyes, 2004), specifically BiCG-Stab method (Van der Vorst, 1992), since the system is non-symmetric. This has the added advantage of only relying on matrix-vector multiplies of the gradient of F.

We also considered approximating the inverse via a polynomial $P_n(\nabla_H F)$, using the geometric series $P_n(x) = 1 + x + x^2 + \ldots + x^n$, which converges provided that $||\nabla_H F|| < 1$. With $n = 1$, this proved a reasonable approximation for Part-of-Speech tagging (Section 3.2). For other tasks, however, we found the eigenvalues were not as well-behaved with this approximation scheme.

2.4 Gradients

In order to train the model, we perform gradient descent. We take the gradient of the loss function:

$$
\nabla_\theta L = \nabla_\theta \ell + \nabla_H \ell \nabla_\theta H
$$

The gradient of the hidden units with respect to the parameters can found via the implicit definition:

$$
\begin{aligned}
\nabla_\theta H &= \nabla_\theta F + \nabla_H F \nabla_\theta H + \nabla_\xi F \nabla_\theta \xi \\
&= (I - \nabla_H F)^{-1} (\nabla_\theta F + \nabla_\xi F \nabla_\theta \xi)
\end{aligned}
$$

where the factorization follows from the noting that

$$
(I - \nabla_H F) \nabla_\theta H = \nabla_\theta F + \nabla_\xi F \nabla_\theta \xi.
$$

The entire gradient is thus:

$$\nabla_\theta L = \nabla_H \ell (I - \nabla_H F)^{-1} \left(\nabla_\theta F + \nabla_\xi F \nabla_\theta \xi \right) + \nabla_\theta \ell \qquad (1)$$

Once again, the inverse of $I - \nabla_H F$ appears, and we can compute it via Krylov subspace methods.

2.5 Transition Functions

Recall the original GRU equations (Cho et al., 2014), with slight notational modifications:

final hidden	$h_t = (1 - z_t)\hat{h}_t + z_t \tilde{h}_t$
candidate hidden	$\tilde{h}_t = \tanh(W x_t + U(r_t \hat{h}_t) + \tilde{b})$
update weight	$z_t = \sigma(W_z x_t + U_z \hat{h}_t + b_z)$
reset gate	$r_t = \sigma(W_r x_t + U_r \hat{h}_t + b_r)$

We make the following substitution for $\hat{h}_t$ (which was set to h_{t-1} in the original GRU definition):

state comb.	$\hat{h}_t = s h_{t-1} + (1 - s) h_{t+1}$	
switch	$s = \frac{s_p}{s_p + s_n}$	
prev. switch	$s_p = \sigma(W_p x_t + U_p h_{t-1} + b_p)$	(2)
next switch	$s_n = \sigma(W_n x_t + U_n h_{t+1} + b_n)$	

This modification makes the architecture both implicit and bidirectional, since $\hat{h}_t$ is a linear combination of previous and future hidden states. The switch variable s is determined by a competition between two sigmoidal units s_p and s_n, representing the contributions of the previous and next hidden states, respectively.

2.6 Implementation Details

We implemented the iRNN structure using Theano (Bergstra et al., 2011). The product $\nabla_H F v$ for various v, required for the BiCG-Stab method, was computed via the `Rop` operator. In computing $\nabla_\theta L$ (Equation 1), we noted it is more efficient to compute $\nabla_H \ell (I - \nabla_H F)^{-1}$ first, and thus used the `Lop` operator.

Batching the nonlinear solver was slightly tricky – it was straightforward to perform the same BiCG-stab computations across different elements in the batch, but some elements converged significantly faster than others. For this reason, we found it helpful to run BiCG from two separate initializations for each element, one selected randomly and the other set to the forward approximation of the GRU (omitting Equation 2). If either of the two candidates converged, we took its value and stopped computing the other.

3 Experiments

3.1 Biased random walks

We developed an artificial task with bidirectional sequence-level dependencies to explore the performance of our model. Our task was to find the point at which a random walk, in the spirit of the Wiener Process (Durrett, 2010), changes from a zero to nonzero

mean. We trained a network to predict when the walk is no longer unbiased. We generated algorithmic data for this problem, the specifics of which are as follows. First, we chose an integer interval length N uniformly in the range 1 to 40. Then, we chose a (continuous) time $t' \in [0, N)$, and a direction $v \in \mathcal{R}^d$. We produced the input sequence $x_i \in \mathcal{R}^d$, setting $x_0 = 0$ and iteratively computing $x_{i+1} = x_i + \mathcal{N}(0, 1)$. After time t, a bias term of $b \cdot v$ was added at each time step $(b \cdot v \cdot (t' - t))$ for the first time step greater than t'. b is a global scalar parameter. The network was fed in these elements, and asked to predict $y = 0$ for times $t \leq t'$ and $y = 1$ for times $t > t'$.

For each architecture, ξ was simply the unmodified input vectors, zero-padded to the embedding dimension size. The output was a simple binary logistic regression. We produced 50,000 random training examples, 2500 random validation examples, and 5000 random test examples. The implicit algorithm used a hidden dimension of 200, and the b-LSTM had an embedding dimension ranging from 100 to 1000. b-LSTM dimension of 300 was the point where the total number of parameters were roughly equal.

The results are shown in Table 1. The b-LSTM scores reported are the maximum over sweeps from 100 to 1500 hidden dimension size. The iRNN outperforms the best b-LSTM in the more challenging cases where the bias size b is small.

b	iRNN Error	b-LSTM Error
2.0	0.0226	**0.0210**
1.0	**0.0518**	0.0589
0.75	**0.0782**	0.0879
0.5	**0.119**	0.132
0.25	**0.189**	0.205

Table 1: Biased walk classification performance.

3.2 Part-of-speech tagging

We next applied our model to a real-world problem. Part-of-speech tagging fits naturally in the sequence labeling framework, and has the advantage of a standard dataset that we can use to compare our network with other techniques. To train a part-of-speech tagger, we simply let L be a softmax layer transforming each hidden unit output into a part of speech tag. Initially, ξ consisted only of word vectors for 39,000 case-sensitive vocabulary words. Next, we lowercased the vocabulary words, but added a single feature indicating whether case appeared in the data. Third, we added six additional 'word vector' components to encode the top-2000 most common prefixes and suffixes of words, for affix lengths 2 to 4. Finally, we added in other (binary) features to indicate the presence of numbers, symbols, punctuation, and more rich case data, as used by (Huang et al., 2015).

We trained the Part of Speech (POS) tagger on the

Penn Treebank Wall Street Journal corpus (Marcus et al., 1993), blocks 0-18, validated on 19-21, and tested on 22-24, per convention. Training was done using stochastic gradient descent, with an initial learning rate of 0.5, and a batch size of 20. Word vectors were of dimension 200, prefix and suffix vectors were of dimension 12. Hidden unit size was equal to feature input size, so in this case, 280. Training took about 5 seconds per batch on a Tesla K40 GPU.

As shown in Table 2, the iRNN outperformed baselines GRU, LSTM, b-LSTM, all with 500-dimensional hidden layers, as well as the Stanford Part-of-Speech tagger (Toutanova et al., 2003) (model `wsj-0-18-bidirectional-distsim.tagger` from 10-31-2016). Note that performance gains past approximately 97% are difficult due to errors/inconsistencies in the dataset, ambiguity, and complex linguistic constructions including dependencies across sentence boundaries (Manning, 2011).

Architecture	WSJ Accuracy
GRU	96.43
LSTM	96.47
Bidirectional GRU	97.28
b-LSTM	97.25
iRNN	**97.37**
Stanford POS Tagger	97.33

Table 2: Tagging performance relative to other recurrent architectures.

3.2.1 Visualizations

We visualized some of the outputs of the "switch" variables for various sentences. The switch is made up of many features, and it does not necessarily always correspond to human judgment, but by taking the average, one can get a sense of the flow of information. In Figure 3, we see a visualization of the switch on a very simple sentence, and in Figure 4 we see it in action over a more complicated sentence. Interestingly, phrasal structures emerge.

4 Conclusion and Future Work

We have introduced a novel, implicitly defined neural network architecture based on the GRU and shown that it outperforms a b-LSTM on an artificial random walk task and slightly outperforms both the Stanford Parser and a baseline bidirectional network on the Penn Treebank Part-of-Speech tagging task.

In future work, we intend to consider implicit variations of other archetectures, such as the LSTM, as well as additional, more challenging, and/or data-rich applications.
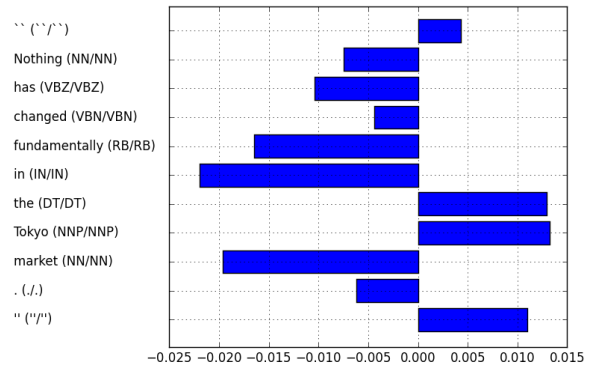
5 Acknowledgements

Figure 3: Visualization of the switch variable, with True/Predicted POS tags. Positive values indicate a right-to-left flow of information, while negative values indicate left-to-right. Note how 'Tokyo' modifies 'market', and information flows between them.
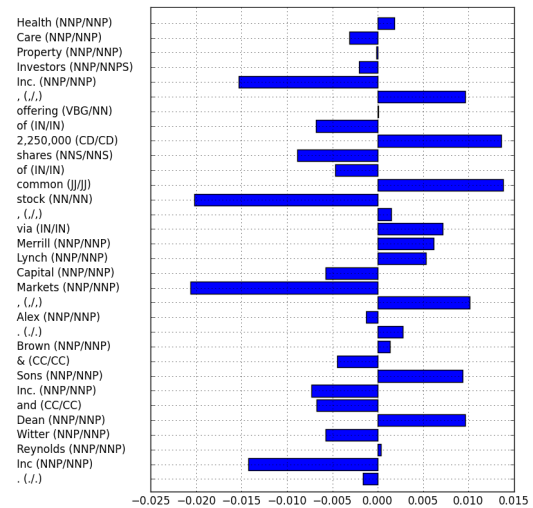

Figure 4: A more complicated example, more representative of the WSJ corpus.

References

James Bergstra, Frédéric Bastien, Olivier Breuleux, Pascal Lamblin, Razvan Pascanu, Olivier Delalleau, Guillaume Desjardins, David Warde-Farley, Ian Goodfellow, Arnaud Bergeron, et al. 2011. Theano: Deep learning on gpus with python. In *NIPS 2011, BigLearning Workshop, Granada, Spain*.

Kyunghyun Cho, Bart van Merriënboer, Dzmitry Bahdanau, and Yoshua Bengio. 2014. On the properties of neural machine translation: Encoder–decoder approaches. *Syntax, Semantics and Structure in Statistical Translation* page 103.

Richard Durrett. 2010. *Probability : theory and examples*. Cambridge University Press, Cambridge New York.

Jenny Rose Finkel, Trond Grenager, and Christopher Manning. 2005. Incorporating non-local information into information extraction systems by gibbs sampling. In *Proceedings of the 43rd Annual Meeting on Association for Computational Linguistics*. Association for Computational Linguistics, pages 363–370.

Alex Graves and Jürgen Schmidhuber. 2005. Framewise phoneme classification with bidirectional lstm and other neural network architectures. *Neural Networks* 18(5):602–610.

Sepp Hochreiter and Jürgen Schmidhuber. 1997. Long short-term memory. *Neural computation* 9(8):1735–1780.

Zhiheng Huang, Wei Xu, and Kai Yu. 2015. Bidirectional lstm-crf models for sequence tagging. *arXiv preprint arXiv:1508.01991* .

Dana A Knoll and David E Keyes. 2004. Jacobian-free newton–krylov methods: a survey of approaches and applications. *Journal of Computational Physics* 193(2):357–397.

Christopher D Manning. 2011. Part-of-speech tagging from 97% to 100%: is it time for some linguistics? In *International Conference on Intelligent Text Processing and Computational Linguistics*. Springer, pages 171–189.

Mitchell P Marcus, Mary Ann Marcinkiewicz, and Beatrice Santorini. 1993. Building a large annotated corpus of english: The penn treebank. *Computational linguistics* 19(2):313–330.

Razvan Pascanu, Tomas Mikolov, and Yoshua Bengio. 2013. On the difficulty of training recurrent neural networks. *ICML (3)* 28:1310–1318.

Lawrence R Rabiner. 1989. A tutorial on hidden markov models and selected applications in speech recognition. *Proceedings of the IEEE* 77(2):257–286.

Mike Schuster and Kuldip K Paliwal. 1997. Bidirectional recurrent neural networks. *Signal Processing, IEEE Transactions on* 45(11):2673–2681.

Kristina Toutanova, Dan Klein, Christopher D Manning, and Yoram Singer. 2003. Feature-rich part-of-speech tagging with a cyclic dependency network. In *Proceedings of the 2003 Conference of the North American Chapter of the Association for Computational Linguistics on Human Language Technology-Volume 1*. Association for Computational Linguistics, pages 173–180.

Henk A Van der Vorst. 1992. Bi-cgstab: A fast and smoothly converging variant of bi-cg for the solution of nonsymmetric linear systems. *SIAM Journal on scientific and Statistical Computing* 13(2):631–644.